www.elsevier.com/locate/memsci

Improved conductivity and anti(bio)fouling of cation exchange membranes by AgNPs-GO nanocomposites

María Irene López-Cázares, Fátima Pérez-Rodríguez, J. René Rangel-Méndez, Marisol Centeno-Sánchez, Luis F. Cházaro-Ruiz

PII: S0376-7388(18)30998-0
DOI: https://doi.org/10.1016/j.memsci.2018.08.036
Reference: MEMSCI16410

To appear in: *Journal of Membrane Science*

Received date: 13 April 2018
Revised date: 10 August 2018
Accepted date: 21 August 2018

Cite this article as: María Irene López-Cázares, Fátima Pérez-Rodríguez, J. René Rangel-Méndez, Marisol Centeno-Sánchez and Luis F. Cházaro-Ruiz, Improved conductivity and anti(bio)fouling of cation exchange membranes by AgNPs-GO nanocomposites, *Journal of Membrane Science,* https://doi.org/10.1016/j.memsci.2018.08.036

Improved conductivity and anti(bio)fouling of cation exchange membranes by AgNPs-GO nanocomposites

María Irene López-Cázares[1], Fátima Pérez-Rodríguez[2], J. René Rangel-Méndez[1], Marisol Centeno-Sánchez[1], Luis F. Cházaro-Ruiz[1*]

[1] *División de Ciencias Ambientales, Instituto Potosino de Investigación Científica y Tecnológica, A.C., Camino a la Presa San José 2055, Lomas 4*a *Sección, San Luis Potosí, SLP, México C.P. 78216.*

[2]*CONACYT - Instituto Potosino de Investigación Científica y Tecnológica, A.C., Camino a la Presa San José 2055, Lomas 4*a *Sección, San Luis Potosí, SLP, México C.P. 78216.*

**Correspondence to.* luis.chazaro@ipicyt.edu.mx)

Abstract

Nafion and Ultrex membranes were modified with nanocomposites (NCs) of silver nanoparticles (AgNPs) immobilized on graphene oxide (GO) as a thin film, using a polydopamine adhesive (pda). The morphological, physicochemical, transport, electrochemical and anti(bio)-fouling properties were determined. The results indicated that the silver nanoparticles were immobilized on adsorption points of the graphene oxide to form nanocomposites. Polydopamine acted satisfactorily as a support and adhesive to bind the nanocomposites to the outer and inner surface of the membranes. The hydrophilicity, ionic exchange capacity, fixed ion concentration, electrochemical and conductivity properties were mostly enhanced in the modified Nafion membranes with pdaGO and pdaNC, but in the Ultrex a shortening of the hydrophilic channels occurred. The impedance results suggested that both modified membranes were more conductive at low frequencies or longer times, due to an adequate interfacial distribution of charges. The differences were attributed to the microstructure of the membranes. Also, the modification of Nafion and Ultrex membranes improved their anti(bio) fouling properties. Hence, both membranes could be used in separation systems, since they allow a higher charge transfer and low energy consumption.

Keywords: modified cationic exchange membranes, silver nanoparticles-graphene oxide nanocomposites, proton conductivity, anti-(bio) fouling properties, and electrical conductivity.

1. 1. Introduction

Ion exchange membranes are used in the selective transport processes of charged particles [1], for example electrodyalisis, capacitive deionization and fuel cell technology, such as bioelectrochemical systems (BES) [2]. Among the BES are the microbial fuel cells (MFCs) and the microbial electrolysis cells (MECs), that do not only generate energy and hydrogen, respectively, but also, it is possible to treat organic wastes to generate value-added products [3].

The most common and efficient arrangements of MEC/MFC are the two chambers cell: an anodic, in which the organic waste is oxidized to H^+ and CO_2 by a bacterial biofilm on the anode, and a cathodic chamber, where the H^+ can be reduced to produce H_2 [3]. Between the chambers there is a separating membrane, which is a protonic/cationic exchange membrane (PEM/CEM), that is considered the most important element of the system because it prevents the mixing of oxidant and fuel [4]. The most used commercial membranes are Nafion (ionomer by Du Pont from 70`s) and Ultrex [5], which are polymers composed by a hydrophobic skeleton and hydrophilic domains, and they also contain sulfonic acid groups [6].

Considering that the fundamental characteristics of an ideal membrane are: permeselectivity, hydrophilicity, good electrochemical properties, homogeneity, mechanical and thermal stability and biofouling resistance [7], the performance of MFC/MEC, so far has been limited due to several problems related with the PEM/CEM, since the latter represents an internal resistor [7]. Additionally, the formation of a (bio)fouling layer that occurs by adhesion of microorganisms (biofilm), organic substrates, particle retention, colloids, salts and other cations that are in concentrations five times higher than protons, such as Na^+, K^+ and Ca^{2+} from nutrient mineral buffer [4]. As a consequence, they affect the transport properties of the membrane, the electrical conductivity, the protonic and cationic permeability, due to the blocking of the proton transport from the anodic to cathodic compartment. As a result, the anolyte is acidified and the catholyte alkalized by deficient proton concentration, generating a pH gradient and a decrease of oxidative microbial activity or death of microorganisms, reducing the MFC/MCEs performance [4]. Until now, these problems have been resolved by adding buffer to the chambers, and for the cleaning/replacement of the membranes, which eventually increases the operating costs [8]. All the above indicates that a solution is to modify PEM/CEM to improve not only its mechanical, physicochemical and electrochemical properties, but also to reduce its (bio)fouling.

Regarding this, blending of polymer chains with nanoparticles (NPs) of organic oxides (such as MgO, CaO, SiO_2, Al_2O_3), clays, zeolites, silicates and Fe_3O_4 have been made, by obtaining an

improvement in the mechanical and thermal properties, but with drawbacks like low conductivity and agglomeration of NPs [9,10]. Until now, the most common methods to improve the physicochemical and electrochemical properties include the blending of an additional charge to obtain a higher water absorption and ion exchange capacity, and the improvement of the conductivity. In the case of the heterogeneous membranes, it is common either to use blending additives or to make a surface modification. Hence, nanoparticles of Ag, zeolite and metal oxides have been added to the membrane solution to improve its conductivity [11]. The membrane surface modification was performed by applying a thin film of surfactants, polyelectrolytes, sulfonamides and conductive polymeric coatings by means of the casting, plasma, coating, electrodeposition, grafting, linkers and immersion methods increases its surface hydrophilicity [11]. Also, the self-polymerization of polydopamine (pda) has been used to transform not only hydrophobic to hydrophilic surfaces, but also the internal structure of the membranes. It is very easy to apply, and not only adheres to universal surfaces but also immobilizes nanoparticles and nanocomposites. In addition, it has been recently found that inhibits the (bio)-fouling [12]. As a matter of fact, pda on ultrafiltration and Nafion membranes have shown microstructural changes and decreasement of the contact angle, charge transfer resistance, methanol crossing and (bio)-fouling [12,13], besides it has been used to adhere nanocomposites that are forming uniform and strong connections.

On the other hand, to improve the physicochemical and electrochemical properties of a homogeneous membrane such as Nafion, organic and inorganic fillers have been added to a membrane solution to modify its surface and maintain the conductivity and interconnectivity in the nanophase, in order to obtain highly efficient hybrid membranes. For which, ionic liquids with phosphoric, sulfonic, phytic and $Ti_3C_2T_X$ groups have been used [14,15]. In studies made by Liu et al. (2016) [16] the authors have been added functionalized carbon nanotubes, graphene oxide (GO) with different degrees of oxidation and size, and functionalized carbon quantum dots with sizes between 2 and 10 nm, in order to ensure that the 2D and 3D compounds can generate layers and line up in the form of sheets, which allow a greater ion conductivity [17,18].

In addition, lately a comprehensive statistical study concerning membrane modifications indicates that the hydrophilic fillers and surface modification simultaneously applied is the best option to improve the physicochemical and electrochemical properties [19].

Concerning the anti-(bio)fouling properties, the membrane surfaces have been altered with polyethylene glycol (PEG), poly(acrylic acid), TiO_2, polyenes and polyamides coatings applied

by plasma. These modifiers change the hydrophilicity and surface charge, triggering anti-fouling properties [20]. Besides, Ag, Cu, TiO_2 and ZnO nanoparticles and lately nanocarbonaceous materials (carbon nanotubes and GO) have been added to poly(acrylic acid) and poly(ethersulfone) (PES) membranes, enhancing their antibacterial properties and improving their conductivity [21–25]. The membranes have been superficially modified by GO sheets and nanocomposites due to its content of a large number of surface oxygenated functional groups, which maintain their negative charge during an extensive pH range [26], so that they attract positive charges, in addition to their high water affinity, high surface area, good chemical and mechanical stability, allowing to obtain highly permeable membranes with good conductivity. In addition, bacterial inactivation by GO has been newly demonstrated [27]. This modification has been made by two procedures: 1) using linkers, e.g. cysteamine, polylisine and fenilendiamine, and 2) assembling layer by layer [21,23,25]. In addition, the pdaGO nanocomposites have showed a catalytic activity in some biosensors [28]. For this reason, pda films have already been used to adhere GO sheets and nanocomposites on membranes improving proton conductivity, the water flux, monoselectivity, antibiofouling, thermal and mechanical properties [28, 29]. Accordingly, if the antibacterial, conductivity and anti-(bio)fouling properties of metallic nanoparticles, GO sheets and pda are adequately combined on membranes, their performance could be improved for future applications. As far as we know, these studies are still missing, so the main objective of this work was to modify in an easy and practical way, commercial cationic exchange membranes, Nafion (homogeneous) and Ultrex (heterogeneous), with nanocomposites of silver nanoparticles on GO (AgNPs-GO) using pda as adhesive. Besides, their morphological, physicochemical, transport, electrochemical and anti-(bio)fouling properties were characterized.

2. Experimental

2.1. Immobilization and characterization of nanocomposites of AgNPs-GO

The nanocomposites (NCs) were prepared according to the following procedure: a solution of $AgNO_3$ (Jalmek P2325-03) (0.1 M) and gallic acid as reducing agent (Jalmek A1925-04) (0.05 M) were employed. Four v/v ratios of $AgNO_3$:GO (graphene oxide in aqueous solution, from supermarket graphene, 6.2 g/mL) were tested: 1:3, 3:1, 6:1 and 9:1 (Ag_1:GO, Ag_3:GO, Ag_6:GO and Ag_9:GO, respectively). As basifying agent, NH_4OH (Jalmek A5325-12) was used. The complete procedure of the nanocomposite synthesis is found in section 2S.1 (see Supplementary Material). The resulting NCs were washed with deionized water (DI) in a

centrifuge Labnet Spectrafuge 6C (model C006) at cycles of 13300 rpm for 30 min, until the pH of the DI was reached. After each cycle, the supernatant was decanted. Then, the solid was dried in an oven (Thermo scientific precision) at 45 °C and then in an Eppendorf vacuum concentrator model vacufuge plus, in order to calculate their yield. The dried solids were kept in a desiccator until their use. Another batch of NCs was maintained in isopropanol (Fermont 06095) until further use to modify membranes.

2.1.1 FTIR (Fourier Transform Infrared spectroscopy) Analysis

The FTIR analysis were made in a Thermoscientific Nicolet 6700 FT-IR at ATR mode (attenuated total reflectance accessory, ATR), at 128 scans, 4 cm^{-1} resolution and wavenumbers between 4000 and 500 cm^{-1}. The data was collected by the OMNIC software.

2.1.2 XRD (X-Ray Power Diffraction) Analysis

The results of XRD were obtained in a Rigaku smartlab x-ray equipment (software PDXL2), using the powder technique, with Cu radiation between 10 and 80º, with a step of 0.06º at 40 kV and 30 mA.

2.1.3 Raman spectroscopy

A Renishaw Invia Raman microscope equipment with an Argon laser at 633 nm was used, and the measurements were at a power of 50 mW, integration time of 5 s at 20 °C, and in a range between 1200 to 1800 cm^{-1}. The data was collected by the XCal-View software.

2.1.4 SEM (Scanning Electron Microscope)

The NCs morphology was observed in a grid (diluted in isopropanol) in a Dual Beam Scanning Electron Microscope (FIB / SEM) FEI-Helios Nanolab 600 at a working distance of 4.2 mm, at 86 pA, and 5 KV.

2.1.5 UV-Vis analyzes

In order to determine the degree of flake stacking of GO, UV-Vis analyzes were performed on a Thermo spectronic Aquamate Lambada 35 series equipment in the transmittance mode from 200 to 900 nm, using a solution of 1 mg of NCs suspended in dimethylphomamide (DMF). The number of stacked layers was calculated considering that each GO sheet in solution absorbs only 2.3% of the light [30].

2.2. Performance of pda as support and adhesive of GO and NCs

The polymerization of dopamine hydrochloride (DA, at 10 mg/mL, Sigma Aldrich H8502) was carried out: 1) without a substrate, just to obtain pda; 2) on GO flakes (previously sonicated); and 3) on the NCs. The polymerization was carried out for 24 hours in a buffer solution (See preparation in Supplementary Material, section 2S.2), pre-bubbled with air for 20 minutes in an ice bath. Afterwards, they were washed

3 times at 10,000 rpm for 15 min, and observed in a grid in a SEM FEI-Helios Nanolab 600 at a working distance of 4.6 mm, at 86 Pa and 5 KV.

2.3. Characterization of membranes with immobilized AgNPs-GO nanocomposites

The commercial cationic exchange membranes Nafion (N) and Ultrex (U) were from a Fuel cell store 1600001-2 and CMI- 7000, respectively. Four different modification methods were tested, considering the influence of DA and NC concentrations and polymerization time. The four methods of anchoring of NCs to the membranes, the three polymerization times and the three DA concentrations, as well as the three NCs ratios used and the hydrophilicity and conductivity measurements are widely described in Section 2S.7 of Supplementary Material, in order to optimize the anchoring, filterability and conductivity properties.

Once the best conditions of preparation of the polymeric films were found, the surface of the commercial membranes was modified. Before that, the Nafion and Ultrex membranes were pretreated (See supplementary material, section 2S.5). The pda was used as an adhesive in 3 different modifications, from 10 mg/mL of DA monomer for 1) pda, 2) 100 µL of GO for pdaGO and 3) 10 mg/mL of NC in isopropanol for pdaNC films. The modifications were made with the membranes immersed into the buffer solutions under agitation during 24 hours of polymerization to avoid the re-stacking of GO sheets. Once the membranes were modified, they were dried at 45 ºC for 24 hours and kept in a desiccator until later use. The characterization included the study of morphological, topographic, physicochemical, transport and electrochemical properties. The morphological and the topographic characteristics were analyzed by SEM and Atomic force microscopy (AFM). For the observations in SEM, the membranes were superficially and transversally cut with a scalpel and coated with Au. The analyzes were carried out at low vacuum and at an working potential of 10 kV in a Quanta 250 microscope. The AFM analyzes were carried out in a JEOL atomic force microscope model JSPM 5200 scanning probe microscope. Silicone AFM probes with the following characteristics were used: resonance frequency of 15 and a constant force of 0.2. The measurements were obtained in contact-mode with areas of 5x5 and 20x20 μm^2. Image processing was carried out in a WSxM 5.0 program and the root mean square (RMS) data of roughness as well as the average height were obtained.

The physicochemical properties, such as hydrophilicity, filterability, ionic exchange capacity (IEC) and fixed ion concentration (FIC) were analyzed. The hydrophilicity and filterability were measured by a dynamic contact angle for 60 seconds in a goniometer scientific instruments (theta litoptical tensiometer) with a oneattension software. The IEC was calculated with Eq. 1, for which, the membranes were maintained in 3 mL of 1 M HCl at room temperature for 24 h, then washed with deionized water. After, they were immersed in 1 M NaCl for 24 h, to exchange the H^+ for Na^+. The final solution was titrated with 0.01 M NaOH and with phenolphthalein as an indicator. The amount of absorbed water was obtained by the difference of weight of the dried membranes and humidified by immersion into DI for 24 h. The water

content % (wc) was calculated with Eq. 2. In addition, from the IEC data and water content, the FIC was obtained with Eq. 3.

$$IEC = \frac{(conc.NaOH)*(vol.NaOH)}{Wdry} \quad \text{Eq. 1}$$

$$\%wc = (\frac{w_{wet}-w_{dry}}{w_{dry}}) * 100 \quad \text{Eq. 2}$$

$$FIC = {}^{IEC}/_{\%wc} \quad \text{Eq. 3}$$

Regarding to electrochemical properties, membrane potentials (E_m), the apparent transport numbers in the membrane and permeselectivity (t_1^m, P_s) were obtained by means of Eq. 4 and 5. A two compartment acrylic electrochemical cells (see Supplementary material, sections 2S.3 and 2S.4) was used, as well as two reference Ag/AgCl/KCl 3M electrodes, one of side of the membrane, under constant agitation. The exposed surface area of the membrane was 0.5 cm^2, which was adjusted with an O-ring in the middle of the two compartments. One compartment contained a 0.1 M NaCl solution, while the other 0.01 M NaCl, allowing the measurement of the potential changes associated with the diffusion of the cations. The measurements were made during 15 min, after a stabilization time of 10 min, using a digital multimeter (Keithley 2110 51/2) and a potentiostat/galvanostat (Bio-logic SAS- model VSP3 controlled by a software EC-Lab version 10.23). The measurements of Donnan's potentials were made in four electrode cells, using two reference electrodes of Ag/AgCl/KCl 3 M, and two graphite electrodes (Ultrapure Alfa Aesar).

$$t1^m = \frac{1}{2}\left[(Em)\left(\frac{RT}{nF}\right)\ln(\frac{a1}{a2}) + 1\right] \quad \text{Eq. 4}$$

$$Ps = \frac{t1^m - t^0}{1-t^0} \quad \text{Eq. 5}$$

R, ideal gas constant

T, temperature

n, the valence of counter ion

a1 and a2 are the electrolyte activities

t^0 is the transport number in solution for Na^+

The internal resistances/conductivity of the membranes were obtained by current interruption (CI), every 10 sec, and with a compensation of 80%, and by potentiostatic electrochemical impedance spectroscopy (PEIS) at 100 KHz, 10 mV and 85% compensation. Additionally, the limiting current (I_{lim}) was obtained by means of linear sweep voltammetry (LSV) at a sweep rate of 0.25 mV s^{-1}, in a potential range from of open circuit potential (OCP) to 1.5 V. A two compartment cell with two Ag/AgCl/KCl 3 M reference electrodes and two Ti/Pt plates for the internal resistances/conductivity measurements. For the limiting current measurements two Pt mesh electrodes were employed instead of the Ti/Pt electrodes. An electrolytic solution 0.01 M NaCl was used in both cases.

The measurements of membrane transport processes were carried out by EIS, at OCP between 100 KHz and 10 mHz, with 6 points per decade at 10 mV of amplitude, in a potentiostat/galvanostat model VSP3 Bio-Logic SAS coupled to EC-Lab software version 10.23, the tests were made in acid (0.1 M H_2SO_4) and

neutral (0.5 M NaCl) media. A conventional three-electrode cell was used, where the modified membranes were considered as ionic solid conductors and were used as working electrodes (WE), with a Pt mesh as a counter electrode (CE), and the Ag/AgCl/KCl 3 M and $Hg/Hg_2SO_4/K_2SO_4$ sat. systems as a reference electrode (RE) for neutral and acid media, respectively (See experimental arrangement in the Supplementary material, section 2S.6). In addition, the fitting of the experimental Nyquist diagrams to an equivalent circuit was performed using the Z-view software, which allowed to obtain the resistances of membrane-solution contact R_{m+s} and the interfacial resistances, $[(R_{EDL}+Rd_{DB})-R_{m+s}]$, as well as the calculation of their conductivities at early and longer times by mean of Eq. 6.

$$\sigma = \frac{L}{R_m A} \qquad \text{Eq. 6}$$

Where R_m is the resistance, L is the thickness (cm) and A is the effective area of the membrane (cm^2).

2.4. Determination of the anti(bio)-fouling properties

To determine the anti-(bio) fouling capacity, 0.6 cm^2 of the pristine and modified membranes were immersed in an anolyte aliquot (0.5 mL/cm^2) of a microbial fuel cell that was inoculated with municipal wastewater, during 8 hours at room temperature. Then, they were removed and rinsed with phosphate buffer (pH 7). Next, the membranes were fixed with a 4% formaldehyde solution. Subsequently, the membranes were dehydrated at 4 °C for 15 minutes in different ethanol dilutions at 30, 40, 50, 60, 70 80, 90 95 and 100%. Finally, they were stored until they were used in a desiccator at room temperature. For their observation in 3, the membranes were coated with Au and analyzed at low vacuum and at a working potential of 10 kV in a Quanta 250 microscope.

3. Results and discussion

3.1 Immobilization and characterization of nanocomposites (NCs)

The SEM micrographs of Fig. 1(a) showed the silver nanoparticles (AgNPs) with a spherical shape between 20 and 40 nm, and the characteristic flake of GO (Fig. 1(b)). Figs. 1(c-f) display the micrographs of different Ag:GO ratios of the synthesized NCs. It is observed that the AgNPs were successfully loaded on the GO. Their anchoring synthesis, immobilization, good dispersion and nanometric size were adequate not to cover the membrane pores and also to show antibacterial activity [31]. It was observed that at a lower amount of the precursor $AgNO_3$ (Ag_1GO), and very few AgNPs were immobilized. As the amount of $AgNO_3$ increased, the number of immobilized AgNPs increased. The Ag_3GO and Ag_6GO (Figs.

1(d) and (e)) composites presented a good dispersion of NPs. Additionally, there were nucleation points of the NPs on the GO flake, from which can occur generation of aggregates, and these were observed more concentrated in Ag_6GO. Therefore, this proportion seems to be adequate on not forming [31]. However, when the proportion of silver increased to 9 (Ag_9GO), the NPs caused a change of the topography (see Fig. 1(f)) and although their distribution was much better than the other samples and the clusters were smaller without any aggregation, a rough surface is induced. In addition, the AgNPs covered the 2D surface of the GO sheet, which limits the presence and activity of the functional groups affecting the surface hydrophilicity and the transport behavior in the case of the ion exchange membranes, as it was already reported by Huang et al., (2016) [24]. The proportions with better dispersion and decoration on the GO sheet were Ag_3GO and Ag_6GO.

3.1.1 X-ray Analysis

Fig. 2(a) shows the diffractograms of the NCs with different proportions of AgNPs. The plane located at 10.82º was observed, and it is characteristic of the GO because is also associated with carbon based materials. The diffractogram of AgNPs showed peaks at 38, 45, 65 and 78º, which are related to crystalline planes 111, 200, 220 and 311, respectively, and correspond to the silver crystalline grid (e.g. face centered cubic). The same planes have already been observed by other authors [32,33] and it confirms the formation of the nanocomposites with good crystallinity and with adequate immobilization. Concerning the NCs, the 110 plane of the GO (10º) only appears in Ag_1GO, where there is less amount of Ag, i.e. few nanoparticles were immobilized (Fig. 1(a)). However, when the Ag ratio increased, the planes that were associated with the GO were not present. In the diffractogram of Ag_1GO, the GO peak, located at 10.82º with a separation of 8.1 nm, is displaced slightly to a lower value at 10.69º, with a separation of 8.3 nm, which indicates that there is more space between the GO sheets by the insertion of the AgNPs. However, this peak disappeared in diffractograms of Ag_3GO, Ag_6GO, and Ag_9GO nanocomposites, since they became very similar to those of the AgNPs diffractograms. The disappearance of the GO peak does not indicate that there was a chemical reduction, since the reduced graphitic structure peak does not appear between 23-26º. In fact, the graphitic bonds could be masked by the AgNPs loaded on the GO sheets [34]. Hence, there was no reduction of GO by neither NH_4OH nor gallic acid, which only reduced $AgNO_3$ to AgNPs [35]. It is well known that the deprotonated phenolic groups of the gallic acid and the $AgNO_3$, placed on the GO sheets, form an unstable intermediate complex Ag-O. Then, the gallic acid is oxidized to its ketonic form reducing Ag^+ to AgNPs which are loaded on GO sheet. Simultaneously, the ketonic groups can stabilize the AgNPs in such a way that they maintain an approximate

average size of 20 nm [35]. Fig. 3 illustrates the mechanism of the preparation of AgNPs-GO nanocomposites.

3.1.2 Raman analysis

The Raman spectra are shown in Fig. 2(b), and they showed the typical D (1320 cm^{-1}) and G (1570 cm^{-1}) bands of the GO, which are associated with the degree of disorder (breathing mode of κ-point phonons) and the graphite transitions (tangential stretching mode of carbon sp^2 atoms) [36,37], respectively. The spectra of AgNPs showed weak bands at 1385 and 1588 cm^{-1} [38]. The spectra of NCs, presented the bands related with GO, which were more evident in Ag_1GO, but they disappeared when the amount of Ag increased. This behavior has already being reported [36,37], and these results could indicate that the NPs were loaded successfully to GO sheets. Additionally, the I_D/I_G ratio decreased from 1.12 to 0.88 for Ag_1GO and Ag_9GO respectively, and the GO bands were distorted, as the amount of silver increased. According to these results, in the Ag_1GO ratio there is a slight decrease of the D and G bands, which may indicate a minor wrinkle formation on the GO sheet due to the loaded of the few AgNPs. However, in Ag_3GO, Ag_6GO and Ag_9GO composites, there is also a deformation of the GO bands, in fact the spectra are more similar to those of the AgNPs than to those of the GO. This indicates that the resulting of in and out plane vibrations of sp^2-bonded carbon are being masked by the AgNPs deposited on the GO sheets, as more Ag is added, more GO surface is covered, and this suggests that there is not an ionic interaction between GO and AgNPs [39].

3.1.3 FT-IR Analysis

Fig. 2(c) shows the FT-IR spectra of the nanocomposites. In the IR spectrum of Ag_1GO, the bands of the oxygenated groups of GO are present but their intensity is decreased. In the Ag_3GO, Ag_6GO and Ag_9GO spectra the bands associated with the oxygenated groups of the GO are mainly attenuated, specifically those for the C-O (1000 and 1400 cm^{-1}), C=C (1628 cm^{-1}) and O-H (3427 cm^{-1}) bonds, which are on the surface of the GO sheet. In contrast, the band at 1740 cm^{-1} associated with C=O groups at the edges of the GO sheet is not weakened, and this supports the evidence that the AgNPs are loading on the superficial oxygenated groups of GO, and not on those at the edges [40].

3.1.4 UV-Vis analysis

Fig. 2(d) shows the number of stacked GO sheets determined from the UV-Vis analysis. A greater amount of Ag increases the number of stacked layers of GO, which was lesser than 10 only in Ag_1GO, Ag_3GO and Ag_6GO composites, which ensure a suitable exfoliation and stabilization of the GO sheets, and with this a two-dimensional structure is maintained which in turn prevents the restacking of the GO layers [30]. However, in the case of Ag_9GO, the stacking was significantly higher, even though if it was expected that the repulsion forces increased with

the increasing number of Ag ions on the surface of GO, which can exfoliate and stabilize the GO sheets [41]. The increasing proportion of AgNPs deposited on the GO flake up to the Ag_6GO composite, causes a repulsion between the GO sheets that exposes the functional groups to the solvent facilitating their ionization, and hence there is an electrostatic repulsion between the negative charges of the stacked sheets surface of GO, but in the case of Ag_9GO composite, most of the functional groups are covered by AgNPs, which facilitates its re-stacking [39].

These results allowed to determine the most appropriate Ag:GO ratio in the NC which was Ag_6GO for the following studies.

3.2 Characterization of the modified membranes

The successful adhesion of pda onto the GO flake and the NCs was examined by SEM and FTIR, which suggested that the pda is a good support and adhesive. Besides, all the modified membranes had an apparent brown color characteristic of the pda coating (see, Supplementary material, Figs. S7, S8, S9). In general, the micrographs showed that just the pda layer agglomerates itself. Otherwise, with the GO flake it is covered and thickened. Besides, the polymerized pda with the NCs covered the GO sheet with the immobilized AgNPs. In the FTIR spectra (see Supplementary material Fig. S9), of GO and NC the bands between 1000 and 1500 cm^{-1} from C-O of the epoxy groups were attenuated in the presence of pda, which suggests a covalent bonding between GO and pda [42]. Besides, the bands between 1524 cm^{-1} (shearing of N-H bonding) and 1621 cm^{-1} (overlapping of C=C and N-H bending) are predominantly indicating the existence of a pda film. Hence, the infrared results indicate that DA has polymerized on the surface of NCs and GO, since the bands associated with the oxygenated groups of GO are attenuated, and only those of pda predominate. The reason is that the DA polymerizes on any substrate, due to its free electrons in resonance. But in the presence of oxygenated groups of GO there is a nucleophilic addition between the ketonic groups of DA quinone (obtained after the oxidation of catechol ring) and the epoxy groups of GO, and a condensation reaction between ketonic groups and carboxylate groups resulting in available OH groups of pda, as indicated by some recent reports that some pda lies between the GO sheets and NCs as a "sandwich filling" generating a strong interaction [43].

In addition, the optimal conditions of DA concentration and polymerization time were determined at 10 mg/mL and 24 h respectively, in order to obtain the highest filterability of water, which was characterized by the lower contact angles values of the modified Nafion and Ultrex membranes, at ~60º and 23º, respectively (see Supplementary material Figs. S10 (a) and (b)). Furthermore, an optimal content of nanoparticles must be determined to avoid the inaccessibility of ions through the membrane [44] and the adequate amount of NC in the polymeric matrix, in order to obtain the highest conductivity was 10 mg/mL (see Supplementary material Fig. S10 (c)).

3.2.1 Morphology, topography and homogeneity studies

The superficial and transversal micrographs of the modified membranes are presented in Fig. 4. The surface of the pristine membranes (Figs. 4(a) and (e)) was mostly smooth and only some particles of mineral salts from the buffer after the synthesis of pda were observed (red arrows). When the pda film is present (Figs. 4 (b) and (f)), the topography of the membranes changed and some aggregates of pda appeared, especially on Ultrex (yellow arrows). When the pda was prepared in the presence of GO, the resulting surface was homogeneous, and there were no pda aggregates (Figs. 4 (c) and (g)); but in comparison with the pristine membranes, the surface became rougher, and the layer thicker and more homogeneous, as it has been seen in other studies [28]. The adhesion of pda to GO demonstrates its capacity of adhesiveness and support. When the pda contains NCs, the resulting polymer film adhered well to the surface of the membranes (Figs. 4 (d) and (h)) and presented a homogeneous distribution of the immobilized AgNPs on GO. Accordingly, the pda coating seems to be uniform, as it has been seen in similar recent studies [45]. This advantage could improve the electrochemical properties of the modified membranes because it will allow an even distribution of current lines of through membrane surface [44]. On the other hand, it is observed in the transversal micrographs (Figs. 4 (a´-d´) and (e´-h´)), that the modification caused internal changes of roughness, also few AgNPs were observed inside the membranes, which could introduce additional charge [11]. There were no significant differences observed between the different modifications. However, those modifications can influence the distribution of the electric current produced by transported ions and the filterability of the membranes as well. The inner changes of the pda are due to three-dimensional interconnections inside the channels, which compacted the pores and caused microstructure changes [45], which makes the membranes superfiltrable and permeselective, and according to Yang et al., 2012 [46], also it could eventually improve the mechanical strength.

According to the results, the modification of the membranes has occurred in the outer and inner surface, in such a way that the flakes of GO and the NCs covered by pda behave as a thin surface film with available O-H groups and additional charge in the case of membranes with silver (pdaNC); whereas in the interior the greater modification happened by the pda, which contributed with O-H and N-H groups, which provide an additional charge.

Fig. 5 and Table 1 show the results of an AFM analysis in order to study the topographic properties. It is observed that the Nafion pristine membrane has a smooth surface and low roughness, but when it is modified with pda there is a significant increase in roughness and height. This, in fact, happened because the agglomerates of coating of pda remain on the surface [29], which is consistent with the results of SEM. When the GO sheets are adhered to Nafion by means of the pda coating, the roughness and height

values are increased, which occurs due to the formation of some GO clusters at the surface level and in the interior to achieve a hybrid membrane [23], similar to those obtained by Li et al., (2016) [17]. By adhering the NCs, it is evident that the roughness and the height decreased considerably, generating smooth surfaces, as it was already observed [47], which is beneficial to obtain anti-fouling surfaces.

Conversely, the modification was very different in the Ultrex membranes since they presented heights in the order of μm, in comparison with the Nafion heights in the order of nm. For the pristine membranes, a smooth surface and some polymeric fibers are observed, as it can be confirmed in the SEM micrographs (see Supplementary Material, Fig. S6). In the control with just pda, the roughness increased only slightly, but the height decreased, which supports the idea that the DA molecules went to between the pores to polymerize mostly inside the membrane [47], not forming a rough coating of pda. If GO and NCs are present, the roughness and height decreased slightly. The above indicates that the modification was carried out more internally, since the modifiers could have spread among the large number of pores, as it was observed in differences of the scattering of light in one and another membrane (Fig. S11). Although the fact of obtaining smoother surfaces can contribute to anti-biofouling, according to recent studies [21,47]. Therefore, this confirms that the modification occurred in a different way, even though the modifiers were the same, and this is due to the different topographies, microstructures and thicknesses of the membranes.

3.2.2 Physicochemical properties

3.2.2.1 Filterability capacities

The contact angles indicated the tendency to wet the membranes. For the modified Nafion membranes the contact angle decreased to <90° (where the hydrophilicity limit is defined) and increased in the following order pdaNC<pda<pdaGO (From 90º to 48, 55 and 62º, respectively). Whilst in Ultrex increased in the following order pda<pdaNC<pdaGO (From 78º to 19, 35 and 40º, respectively) (see Figs. 6(a-c) and Table 2). With just the pda as modifier, all the membranes became superfiltrable, as it has been reported by Yang et al., (2012) [46], where they produced superhydrophilic, functional and porous membranes. Therefore, the proton transport was not blocked due to the pda coatings, on the contrary, more filterable membranes were obtained, since it is expected a decrease of the energy barrier for the proton jump through the Grotthuss mechanism, according to He et al., (2014) [48]. When the GO is present, the surface of the membranes is more hydrophobic. Instead, the decreased observed with NPs, indicated that they did not blocked the channels and increased the hydrophilic character due to the electrical charge that they introduced [49]. The pda that adheres both inside and outside the membrane causes a greater affinity for water. When GO sheets were added the hydrophobic character increased due to the partial chemical reduction of its functional groups via covalent

bonds with the pda, as it has been explained in section 3.2, and by the possible formation of some small aggregates of GO on the surface. But this effect is reversed by the presence of AgNPs that are ionized in aqueous medium and become active sites to adsorb water.

3.2.2.2 Percentage of water uptake measurements

In Table 2, it is shown that the percentage in water content increased in all modified Nafion membranes, indeed this percentage did increase in the following order pdaGO<pda<pdaNC (from 40 to 63, 73 and 78%, respectively). This indicates that there are more connection between the channels to favor the ions transport, that would guarantee a good proton conductivity, which also would be correlated with a higher concentration of fixed groups [50]. In contrast, in the modified Ultrex membranes there was a decrease of absorbed water (From ~36% in pristine membranes to 23% in modified membranes). Only a more significant increase was observed with NCs (up to 25%). The decrease in water absorption indicates that there are fewer open routes and that the voids and cavities that are inside the membrane are not continuous [49].

Therefore, the hydrophilicity/filterability and water absorption were improved in modified Nafion membranes, contrary to what occurred with the modified Ultrex membranes. In comparison with other studies with pda, where the water uptake has been reported between 10 and 40% [13], in this study it was higher (up to 78%), which could improve the conductivity because the superficial charge would become more negative due to the deprotonation of phenolic groups of the pda coating, in addition to the possible charge of the AgNPs that caused more swelling, as it has been reported by Kim et al., (2014) [12] and Porozhnyy et al., (2016) [49]. In this sense, a high amount of additional charge causes high water absorption/retention and swelling due to the continuity (homogeneity) of the modified membrane that allows the connection inside making short-range channels. The decrease of water absorption in Ultrex is due to plugging or low connectivity of “dead ends” channels, as a result of a discontinuity of phases, since this is a heterogeneous membrane, and also due to the presence of an inert part that does not absorb water, but an improvement of the selectivity could be anticipated [13].

3.2.2.3 Fixed ion concentration and ion exchange capacity measurements.

The fixed ion concentration (FIC) and the ion exchange capacity (IEC) are reported in Table 2. The values of both parameters increased in the modified Nafion membranes, and increased in the following order depending on the modifier pdaGO<pda<pdaNC (IEC from 2 to 3.8, 4 and 6 meq/gr and FIC from 6 to 6.8, 7 and 8, respectively). The IEC increased because it improves the number of accessible functional sites, which made the internal membrane-electrolyte

interaction easier, to later improve the ionic transfer and permeselectivity [51]. Though, in the modified Ultrex membranes only the properties of FIC were improved in the following order of modifiers pdaNC<pda<pdaGO (For FIC from 4 to 4.2, 5.3, 5.6 meq/g, respectively), which could be related to the lower swelling and water absorption, caused by the low number of active sites or functional groups connecting the “dead ends” between the inert and active phase of this heterogeneous membrane [16].

The foregoing behavior could influence later on membrane properties and transport characteristics, in accordance with Kamcev et al., (2017) [52] and Ariono et al., (2017) [44]. These differences in behavior can be explained from a point of view of the different microstructure and thickness of the membranes; e.g. Nafion is homogeneous, since it is composed by only one polymer, it is thinner, it has a smooth surface and it has a small pore size, and for these reasons it seems to be more susceptible to be modified successfully [44]. In contrast, the heterogeneous Ultrex is composed by a 50-60 wt% inert gel polystyrene crosslinked with dyvinilbencene, it is thicker, it has a rough surface and it is very porous (Fig. S6). Therefore, the resulted disposition of fixed charges in Nafion is more homogeneous and reachable, while in Ultrex the modifications are more heterogeneous, with their inner channels blocked by an inert part, causing inaccessibility of the functional groups [53].

In addition, the modification by pda can be made in different ways, depending on the difference of microstructures, for example in a thick and porous membrane such as Ultrex, DA molecules enter the interior from where they polymerize and only a small part would remain on the surface, few hydrophilic groups will be in this place, hence in conjunction with the inert part, disruption of the skeleton and its rigid structure has produced low absorption of water. However, in Nafion, which is a thin membrane with a small pore size, most of the DA on the surface until they have polymerized, reaching a highly hydrophilic surface capable of absorbing a large amount of water, due to the arrangement and availability of fixed charges, i.e. more ionic groups are present, continuous nanophase and the formation of short-range channels, in addition to having a more flexible structure.

3.2.3 Electrochemical behavior of modified ion exchange membranes

3.2.3.1 Membrane and Donnan´s potential: Ion mobility of the modified membranes

The electrochemical properties of the modified membranes were also analyzed. The transport of the more mobile ions from one side to another up to a balance causes a potential difference defined as membrane potential. The boundary conditions between the ratio of the counter-ions

in the membrane skeleton and co-ions in the solution determines the Donnan´s potential, and both parameters are related with the structural inhomogeneity [44,54].

Table 3 shows that the membrane potential, transport number (t^1m), permeselecivity (P_s) and Donnan´s potentials were increased in the modified Nafion membranes according to the following order pda<pdaGO<pdaNC, and it was more significant with the NCs contained in pda (e.g. for membrane potential from 30 to 50 mV; t^1m from 0.74 to 0.9; P_s from 0.6 to 0.85 and Donnan´s potential from -0.25 V to -0.08 V). That is, the transport of mass by diffusion and migration improved with the modifications. The enhance indicates that more mobile ions diffuse from the more concentrated to a more dilute solution, indeed because there is a high concentration of fixed groups available (Section 3.2.2.3), what lead to an improvement of the Donnan´s potentials. This effect [55] indicates that there is a higher concentration of ions attached to the gel phase of the polymer [54], and for this reason there was an increase of IEC, FIC, % of water uptake and filterability; and therefore an increase in the permeselectivity [53].

Instead, the physicochemical properties of the modified Ultrex increased as follow: pdaNC<pda<pdaGO (for membrane potential from 50 to 58 mV; t^1m from 0.9 to 0.99 and P_s from 0.84 to 0.98), and it is important to mention that these parameters diminished in the presence of NCs. However, Donnan's potentials were increased not significantly for all modifications (from -0.04 V to -0.12 V), being lower with NCs (up to -0.085 V). The previous behavior appears to be related with the heterogeneous microstructure of Ultrex, which influences its modification and affected its transport properties, in addition to the incorporation of NPs [53,56].

In general, the electrochemical and transport characteristics were improved for all modifications of Nafion, they were significantly higher when the NCs were added [51]. The presence of GO and NCs increases the number of additional sites (OH^-) and the surface charge, so that the conduction of the counter-ions increases, while the repulsion of co-ions is decreased. Besides, the incorporation of pda and pdaGO increased the formation of hydrogen bridge bonds and did not block the transport [28].

3.2.3.2 Internal resistance: Ionic conductivity of the modified membranes

A low membrane resistance is beneficial because it will allow a high conductivity and lower electrical losses [1]. The internal resistance values (IR) or ohmic drop analog to R_{m+s} from EIS, of the modified membranes, determined by PEIS and CI are presented in Table 3. The values associated with modified Nafion membranes decreased in the following order

pda>pdaNC>pdaGO (from 26 to 15, 13.5 and 3.5 ohms/cm^2, respectively). Nevertheless, for the modified Ultrex, the IR increased when the modifiers were added in the following order pda<pdaGO<pdaNC. This behavior is congruent to that observed for R_{m+s} estimated by EIS (Section 3.2.4). This tendency agrees well with the electrochemical and physicochemical properties determined previously.

The conductivity of Nafion increased (see Table 3) with pda and pdaNC<pdaGO (from 12 µS to 23 for pda and 24 < 84 µS for pdaNC<pdaGO, respectively), which indicates a higher ions pathway because the Grotthuss mechanism is preferred [6], and it will guarantee a higher ion transfer and lower power consumption, then higher power densities in a two chamber cell could be obtained [1] (Figs. S15). Therefore, the modification on Nafion was successful, obtaining nanohybrid membranes with continuous short-range channels that form dynamic transport networks.

The increase of IR of modified Ultrex may be due mainly to the increase in thickness (0.056 cm), heterogeneity and tortuosity inside the membrane, which would cause a tortuous way to be crossing by the counter-ions [57], since for being a heterogeneous and thicker membrane than Nafion there is a great separation of phases in the interior, besides the presence of the inert polymer, which causes a separation of nanophases, even after the modification, and the channels that connect the “dead ends” to the proton transport are longer. However, this behavior would only occur at short times, when the membrane has the earlier contact with the solution, but at longer times, the ions can be attracted by the AgNPs, and the connectivity prevails over the disruption of the skeleton and phase separation, since the channels connect more “inert ends”, thus by making the distances shorter for proton transport, it will be possible to carry more charge through the membrane. This can be explained by a conductivity-microstructure relation on the basis of the micro-heterogeneous model [56], e.g. the modifications on Nafion were homogeneous and the fixed groups were accessible, so that there was a higher current flowing through a homogeneous intergel phase. However, Ultrex has a large inert part and the modification was unleveled, so the functional sites result inaccessible and there were shorter ions pathways which provoked a low conductivity [53,54].

3.2.3.3 Determination of limiting current range

Among the applications of modified membranes in separation processes, capacitive deionization is one of the most important, where the flow of ions occurs under the influence of an electric field. Table 3 shows the limiting current values obtained from anodic polarization curves of the modified membranes. It is observed that the limiting current (I_{lim}) increased and shifted towards negative potentials for both modified membranes. This behavior results more important in membranes with pdaGO and pdaNCs, compared with the modified with pda. In fact,

the polarization curves (see Supplementary material, Fig. S12) obtained for the pda coating are constantly flat, due to a limitation in the current flow. This is a consequence of the presence of the pda coating, which in normal conditions in aqueous solution has surface hydrophilic OH groups, but under the influence of a potential field, these groups can be in their quinone oxidized form, which limits the transfer of counter-ions. Whereas with GO and NCs, the curves showed a fast increase in current or constant current flow, which suggests that the ions transport was greater, due to a simultaneous mass transport by the electro-diffusion and electro-convection processes. Therefore, the potentiometric curves suggest that by increasing the applied current, the transition time becomes shorter in the modified membranes with GO and NCs. It has been seen that the current distribution through the homogenized intergel phases made it possible to use the membranes at higher current densities in an ionic separation process, such as capacitive deionization [56,58]. Hence, it suggests that less energy is needed to transport a higher charge density through the modified membranes with GO and NCs because they became more conductive [59].

3.2.4 Electrochemical properties in membrane transport processes

The previous measurements were done by a direct current, but it was not possible to obtain the interfacial resistance at nanometric scale considering the micro-heterogeneous model. To distinguish the phenomena occurring at different times as in the case of modified Ultrex membranes [60]. The membranes were considered as a solid ionic conductor in contact with the electrolyte. In Fig. 7 the Nyquist diagrams of the modified Nafion and Ultrex membranes in acid (a and b) and neutral (c and d) media are presented (see the corresponding Bode diagrams in Supplementary material Figs. S13 and S14). Figs. 7(a) and (c) show that in the limit of high frequencies it is observed that the resistance of the interface membrane-solution, R_{m+s} decreased (close up in Figs. 7 (a) and (c) and Figs. 8(a) and (e)) for modified Nafion, and in the limit of low frequencies their corresponding interfacial resistances (Rinterfacial) associated with the electrical double layer, R_{EDL} and diffusion layer, R_{DBL} decreased, especially for membranes modified with pdaNC and pdaGO. This behavior is more remarkable in neutral than in acid medium. Therefore, the membrane and interfacial conductivities were increased in both working conditions (Figs. 8(c) and (g)). Furthermore, the Nyquist diagrams for the modified Ultrex membranes are also shown in neutral and acid medium (Fig. 7 (b) and (d)). Also the close up of the Nyquist high frequencies, R_{m+s} are shown, and these increase for all the modified membranes (Figs. 7(b) and (d) and Figs. 8(b) and (f)), this, indeed is related with the decrease of attached groups or accessible into the intergel phase, which is due to increase of the

thickness and heterogeneity (discontinuity of nanophases) of this membrane in comparison with Nafion, as it has been reported [57]. However, at low frequencies (or longer times), the interfacial resistances (Rinterfacial) decreased (Figs. 8(b) and (f)) in both media: pdaGO>pda>pdaNC in neutral media and mainly for pdaNC in acid medium. Hence, that the interfacial conductivities are increased for both media (Fig. 8(d) and (h)). This indicates that the channels within the modified Ultrex membrane at longer times have already connected the "dead ends" between the active and inert polymer, so the separation of the nanophases is lower and the conductivity increases. This does not happen with Nafion, since its microstructure is homogeneous and the connection of channels occurs at the first contact with an aqueous solution. This suggests that over a longer period of time there is an increase in interfacial distribution, improving the conductivity properties [1]. In addition, it is evident that in neutral medium there are two time constants in the Nyquist diagrams (Fig. 7(d)), one at high frequencies, related with faster processes, and another one in the low frequencies associated with slower process. The first could be associated to the phenomena of the charging of the electric double layer (EDL) and the second one to the development of the diffusion layer (DBL), respectively.

By using the membranes as electrodes directly, it was possible to evaluate the dispersions in conductance at the interfacial level, as it has already been done recently with other authors [61]; however, the conductivity values were lower (Figs. 8(e,f) and (g,h)), since they are those of interfacial phases inside the pores [62], in comparison with similar conditions in two compartment cells [57].

3.3 Transport processes in the modified membranes

The results suggest that in the modified membranes, the GO flakes and the NCs covered by pda are mainly adhered on the surface forming a thin film, while the pda modifies the surface and the interior of the membranes.

The differences observed in the behavior of each membrane are associated mainly to the internal microstructure and their thickness, as already mentioned. The NCs and GO improved the internal humidification of the homogeneous and thinner Nafion membrane, forming an adequate connection of internal channels composed of a gel phase where there are available fixed groups and an intergel phase, in which the ion transport can be carried out faster, by improving the conductivity properties at early and later times for protons and cations, as it was suggested by the electrochemical impedance measurements.

Therefore, this suggests that the superficial silver could be ionized from AgNPs in aqueous medium, having an acid, hydrophilic and adsorption character, allowing the adsorption of water, increasing the charge density and the transport of counter-ions through the intergel phase. In addition, the semielasticity of the pore walls have been influenced [63]. However, the modifications of Ultrex, even though they improved the attraction of counter-ions, did not favor the connectivity of the internal channels or the availability of the fixed groups, which is mainly associated to the macro and micro-heterogeneous structure of the membrane, and to the existence of an inert phase that makes the ion transport slower in the interior, besides that the membrane is thicker and the transport routes are more tortuous and longer. Unlike the Nafion, in Ultrex the AgNPs, despite being hydrophilic and charged, the structure of the pore walls of this membrane could be more rigid, in such a way that the NPs blocked the channel making the ion transfer slower, decreasing the conductivity at early times. However, the impedance measurements suggested that at longer times the conductivity can be improved, which occurs when an adequate connection between the gel, intergel and inert phases or “dead ends” is reached, since the inert parts were modified by conductive domains of GO and AgNPs. This could be expected, since in general, the heterogeneous membranes have shown low electrochemical properties and a good mechanical strength.

3.4 Anti-(bio)fouling properties of the modified membranes

In Fig. 9, it is observed that the pristine Nafion and Ultrex membranes (Figs. 9(a) and (b)) have bacteria adhered to the surface, even in the Nafion membrane the possible presence of bacteria is observed. However, in the membranes that were modified with pda (c and d) very few bacteria were perceived on the rough surface characteristic of this modification. In fact, this indicates that this modification improved the anti-adhesive properties [12]. Likewise, in the membranes with pdaGO and pdaNC there were no bacteria attached on the roughest surface of the membrane. Indeed, this coincides with the fact that the GO and the AgNPs (Figs. 9(e) and (f), (g) and (h)) have antibacterial capabilities by different mechanisms, in addition to the anti-adhesive properties of the pda [28]. In pdaNC there were only some points of salt from the buffer and the mineral medium in which the inoculum was present, as indicated by the EDAX results inserted in Fig. 9(g).

3.5 Applications of modified ion exchange membranes

The results suggest that the modified membranes can be employed in separation systems, such as microbial fuel or electrolytic cells and in capacitive deionization processes, since the modified membranes allow a high charge transfer with or without the influence of an electric field, in addition to their anti-(bio)fouling properties.

Therefore, the following evaluations of long-term operation are provided. The performance of the membranes as a function of the frequencies (1/t) was analyzed by impedance measurements made in a two-compartment cell. This type of analysis gives an idea of the

behavior of the interfacial properties of the membranes as a function of time. In the range of high frequencies is possible to determine the early contact of the membrane with the solution. At medium frequencies, the behavior of the double electric layer is analyzed. Meanwhile, at low frequencies is possible to determine the pass of current transported by the counter-ions. The Nyquist diagrams shown in Fig. S15 (a) and (b) suggest that at low frequencies or at longer times, the resistance to the charge transfer decreased significantly in the modified membranes.

Hence, the values of power and current densities produced by microbial fuel two-compartment cells with pdaNC modified membranes in long-term operation during 6 months are shown in Figs S15 (c) and (d) and Table S2. The anodic compartment included phosphate buffer, municipal residual water as inoculum, volatile fatty acids as substrate and graphite cloth as an anode, while the cathodic side only contained phosphate buffer and a cathode of graphite felt. The data given in Table S2, showed a higher performance of the microbial fuel cells with modified membranes (400 and 130 mW/m^2 for UpdaNC and NpdaNC, respectively) than those with membranes without pdaNC modification (90 and 70 mW/m^2 for Uctrl and Nctrl, respectively).

Chemical stability and mechanical strength are other important properties, so long-term stability studies were carried out (Fig. S16). The results showed that the modified membranes presented less percentage of weight loss compared to the pristine ones. Therefore it is suggested that the modification allowed a lower diffusion of oxygen inside and therefore a greater resistance and stability.

4. Conclusions

The cation exchange Nafion and Ultrex membranes were satisfactorily modified with polydopamine, as support and adhesive, containing AgNPs-GO nanocomposites. The modifications caused changes in the surface by thin film nanocomposites (pdaGO and pdaNC) and inner surface (only by pda) of the membranes, e.g they became rougher, thicker and more conductive due to the presence of the nanocomposites into the pda. The pda behaved as a reducing agent and adhesive of the GO sheets. All the modified membranes improved the anti(bio)-fouling properties. The modified Nafion membrane improved its hydrophilicity, filterability, water absorption, ion exchange capacity, fixed ion concentration and electrochemical properties. However, the modified Ultrex membrane only improved its hydrophilicity, filterability and density of fixed groups, but its conductive properties were not enhanced at early times. These properties were associated to the fact that the Nafion membrane is homogenous and thinner and therefore allows an adequate interconnection of channels (continuous nanophase), which favors the transport of the charged ions through the intergel phases. Whereas the Ultrex membrane is heterogeneous and thicker, and the interconnection of channels (discontinuous nanophase) made a slower transport of charged ions, due to the presence of an inert polymer that makes the path more tortuous. Thus these modified membranes can be a good option for their use in separation systems such

as bioelectrochemical systems and capacitive deionization since they allow a high charge transfer and low energy consumption.

Acknowledgments

This work was financially supported by grant “Conacyt-SENER Fondo de Sustentabilidad Energética” and “Clúster de Biocombustibles gaseosos” (247006). M. I. López is grateful to SENER-CONACYT for the scholarship received through of **“**CONACYT-SECRETARÍA DE ENERGÍA-SUSTENTABILIDAD ENERGÉTICA 2016-2017 ESTANCIAS POSDOCTORALES EN MÉXICO”. The authors thank D.I. Partida, Guillermo Vidriales, and Elizabeth Cortez for their invaluable technical assistance throughout the investigation. We also appreciate to M.C. Rocha from National Laboratories LAMBAMA and Dr. Gladis Labrada and M.C. Ana Iris Peña from LINAN.

References

[1] A.H. Galama, N.A. Hoog, D.R. Yntema, Method for determining ion exchange membrane resistance for electrodialysis systems, Desalination. 380 (2016) 1–11. doi:10.1016/j.desal.2015.11.018.

[2] Y. Zhang, I. Angelidaki, Microbial electrolysis cells turning to be versatile technology : Recent advances and future challenges, Water Res. 56 (2014) 11–25. doi:10.1016/j.watres.2014.02.031.

[3] D. Pant, A. Singh, G. Van Bogaert, S. Irving Olsen, P. Singh Nigam, L. Diels, K. Vanbroekhoven, Bioelectrochemical systems (BES) for sustainable energy production and product recovery from organic wastes and industrial wastewaters, RSC. Adv. 2 (2012) 1248–1263. doi:10.1039/C1RA00839K.

[4] M. Ghasemi, W.R.W. Daud, A.F. Ismail, Y. Jafari, M. Ismail, A. Mayahi, J. Othman, Simultaneous wastewater treatment and electricity generation by microbial fuel cell: Performance comparison and cost investigation of using Nafion 117 and SPEEK as separators, Desalination. 325 (2013) 1–6. doi:10.1016/j.desal.2013.06.013.

[5] T. Xu, Ion exchange membranes: State of their development and perspective, J. Membrane. Sci. 263 (2005) 1–29. doi:10.1016/j.memsci.2005.05.002.

[6] S.J. Peighambardoust, S. Rowshanzamir, M. Amjadi, Review of the proton exchange membranes for fuel cell applications, Int. J. Hydrogen. Ener. 35 (2010) 93499384.doi:10.1016/j.ijhydene.2010.05.017.

[7] B.E. Logan, B. Hamelers, R. Rozendal, U. Schröder, J. Keller, S. Freguia, P. Aelterman, W. Verstraete, K. Rabaey, Microbial fuel cells: Methodology and technology, Environ. Sci. Technol. 40 (2006) 5181–5192. doi:10.1021/es0605016.

[8] J. Xu, G.P. Sheng, H.W. Luo, W.W. Li, L.F. Wang, H.Q. Yu, Fouling of proton exchange membrane (PEM) deteriorates the performance of microbial fuel cell, Water. Res. 46 (2012) 1817–1824. doi:10.1016/j.watres.2011.12.060.

[9] J. Ramírez-Salgado, Study of basic biopolymer as proton membrane for fuel cell systems, Electrochim. Acta. 52 (2007) 3766–3778. doi:10.1016/j.electacta.2006.10.051.

[10] M. Rahimnejad, M. Ghasemi, G.D. Najafpour, M. Ismail, A.W. Mohammad, A.A. Ghoreyshi, S.H.A. Hassan, Synthesis, characterization and application studies of self-made Fe3O4/PES nanocomposite membranes in microbial fuel cell, Electrochim. Acta. 85 (2012) 700–706. doi:10.1016/j.electacta.2011.08.036.

[11] I.G. Wenten, Recent developments in heterogeneous ion- exchange membrane : preparation , modification, characterization and performance evaluation . Preparation of Heterogeneous IEMs, J. Engin. Sci. Technol. 11 (2016) 916–934.

[12] K.Y. Kim, E. Yang, M.Y. Lee, K.J. Chae, C.M. Kim, I.S. Kim, Polydopamine coating effects on ultrafiltration membrane to enhance power density and mitigate biofouling of ultrafiltration microbial fuel cells (UF-MFCs), Water Res. 54 (2014) 62–68. doi:10.1016/j.watres.2014.01.045.

[13] J. Wang, L. Xiao, Y. Zhao, H. Wu, Z. Jiang, W. Hou, A facile surface modification of Nafion membrane by the formation of self-polymerized dopamine nano-layer to enhance the methanol barrier property, J. Power Sources. 192 (2009) 336–343. doi:10.1016/j.jpowsour.2009.03.014.

[14] J. Maiti, N. Kakati, S. Pil, Y. Soo, Nafion based hybrid composite membrane containing GO and dihydrogen phosphate functionalized ionic liquid for high temperature polymer electrolyte membrane fuel cell, Compos. Sci. Technol. 155 (2018) 189–196. doi:10.1016/j.compscitech.2017.11.030.

[15] Y. Liu, Y. Han, R. Chen, H. Zhang, S. Liu, F. Liang, In situ immobilization of copper nanoparticles on polydopamine coated graphene oxide for H_2O_2 determination, PLoS ONE. 11 (2016) 1–12. doi:10.1371/journal.pone.0157926.

[16] Y. Liu, J. Zhang, X. Zhang, Y. Li, J. Wang, $T_{i3}C_2T_x$ Filler Effect on the Proton Conduction Property of Polymer Electrolyte Membrane, ACS Appl. Energy. Mater. 8 (2016) 20352-20363. doi:10.1021/acsami.6b04800.

[17] P. Li, W. Wu, J. Liu, B. Shi, Y. Du, Y. Li, J. Wang, Investigating the nanostructures and proton transfer properties of Nafion-GO hybrid membranes, J. Membrane. Sci. 555 (2018) 327–336. doi:10.1016/j.memsci.2018.03.066.

[18] W. Wu, Y. Li, J. Liu, J. Wang, Y. He, K. Davey, S. Qiao, Molecular-Level Hybridization of Nafion with Quantum Dots for Highly Enhanced Proton Conduction, Adv. Mater. 1707516 (2018) 1–7. doi:10.1002/adma.201707516.

[19] L. Liu, W. Chen, Y. Li, A statistical study of proton conduction in Nafion-based composite membranes : Prediction, filler selection and fabrication methods, 549 (2017) 393-402 doi:10.1016/j.memsci.2017.12.025.

[20] C. Sun, J. Miao, J. Yan, K. Yang, C. Mao, J. Ju, J. Shen, Applications of antibiofouling PEG-coating in electrochemical biosensors for determination of glucose in whole blood, Electrochim. Acta. 89 (2013) 549–554. doi:10.1016/j.electacta.2012.11.005.

[21] M. Safarpour, A. Khataee, V. Vatanpour, Thin film nanocomposite reverse osmosis membrane modified by reduced graphene oxide/TiO_2 with improved desalination performance, J. Membrane. Sci. 489 (2015) 43–54. doi:10.1016/j.memsci.2015.04.010.

[22] W. Ma, M.S. Rahaman, H. Therien-Aubin, Controlling biofouling of reverse osmosis membranes through surface modification via grafting patterned polymer brushes, J. Water Reuse Desal. 5 (2015) 326-334. doi:10.2166/wrd.2015.114.

[23] H.M. Hegab, A. ElMekawy, T.G. Barclay, A. Michelmore, L. Zou, C.P. Saint, M. Ginic-Markovic, Fine-Tuning the Surface of Forward Osmosis Membranes via Grafting Graphene Oxide: Performance Patterns and Biofouling Propensity, ACS Appl. Mater. Interfaces. 7 (2015) 18004–18016. doi:10.1021/acsami.5b04818.

[24] W. Ma, A. Soroush, T.V.A. Luong, M.S. Rahaman, Cysteamine- and graphene oxide-

mediated copper nanoparticle decoration on reverse osmosis membrane for enhanced anti-microbial performance, J. Colloid Interface Sci. 501 (2017) 330–340. doi:10.1016/j.jcis.2017.04.069.

[25] A. Soroush, W. Ma, Y. Silvino, M.S. Rahaman, Surface modification of thin film composite forward osmosis membrane by silver-decorated graphene-oxide nanosheets, Environ. Sci. Nano. 2 (2015) 395–405. doi:10.1039/C5EN00086F.

[26] J.A Quezada-Renteria, L.F. Cházaro-Ruiz, J.R. Rangel-Mendez. Synthesis of reduced graphene oxide (rGO) films onto carbon steel by cathodic electrophoretic deposition: Anticorrosive coating, Carbon 122 (2017) 266–275. doi:10.1016/j.carbon.2017.06.074.

[27] F. Perreault, A.F. De Faria, S. Nejati, M. Elimelech, Antimicrobial Properties of Graphene Oxide Nanosheets: Why Size Matters, ACS Nano. 9 (2015) 7226–7236. doi:10.1021/acsnano.5b02067.

[28] H.M. Hegab, A. ElMekawy, T.G. Barclay, A. Michelmore, L. Zou, C.P. Saint, M. Ginic-Markovic, Effective in-situ chemical surface modification of forward osmosis membranes with polydopamine-induced graphene oxide for biofouling mitigation, Desalination. 385 (2016) 126–137. doi:10.1016/j.desal.2016.02.021.

[29] L. Shao, Z.X. Wang, Y.L. Zhang, Z.X. Jiang, Y.Y. Liu, A facile strategy to enhance PVDF ultra filtration membrane performance via self-polymerized polydopamine followed by hydrolysis of ammonium fl uotitanate, J. Membrane Sci. 461 (2014) 10–21. doi:10.1016/j.memsci.2014.03.006.

[30] R.R. Nair, P. Blake, A.N. Grigorenko, K.S. Novoselov, T.J. Booth, T. Stauber, N.M.R. Peres, A.K. Geim, Fine Structure Constant Defines Visual Transparence of graphene, Science 320 (2008) 1308. doi: 10.1126/science.1156965.

[31] S. Agnihotri, S. Mukherji, S. Mukherji, Size-controlled silver nanoparticles synthesized over the range 5–100 nm using the same protocol and their antibacterial efficacy, RSC Adv. 4 (2014) 3974–3983. doi:10.1039/C3RA44507K.

[32] L. Huang, H. Yang, Y. Zhang, W. Xiao, Study on Synthesis and Antibacterial Properties of Ag NPs/GO Nanocomposites, J. Nanomater. 2016 (2016)1-9. doi:10.1155/2016/5685967.

[33] I. Roy, D. Rana, G. Sarkar, A. Bhattacharyya, N.R. Saha, S. Mondal, S. Pattanayak, S. Chattopadhyay, D. Chattopadhyay, Physical and electrochemical characterization of reduced graphene oxide/silver nanocomposites synthesized by adopting a green approach, RSC Adv. 5 (2015) 25357–25364. doi:10.1039/C4RA16197A.

[34] H. Begum, M.S. Ahmed, S. Cho, S. Jeon, Simultaneous reduction and nitrogen functionalization of graphene oxide using lemon for metal-free oxygen reduction reaction, J. Power. Sources. 372 (2017) 116–124. doi:10.1016/j.jpowsour.2017.10.035.

[35] G.A Martínez-Castañon, N-Niño-Martínez, F. Martínez-Gutierrez, J.R. Martínez-Mendoza, F. Ruiz, Synthesis and antibacterial activity of silver nanoparticles with different sizes, J. Nanopart. Res. 10 (2008) 1343–1348. doi:10.1007/s11051-008-9428-6.

[36] W. Shao, X. Liu, H. Min, G. Dong, Q. Feng, S. Zuo, Preparation, Characterization, and Antibacterial Activity of Silver Nanoparticle-Decorated Graphene Oxide Nanocomposite, ACS Mater. Interfaces. 7 (2015) 6966-6973 doi:10.1021/acsami.5b00937.

[37] J. Zeng, X. Tian, J. Song, Z. Wei, Green synthesis of AgNPs/reduced graphene oxide nanocomposites and effect on the electrical performance of electrically conductive adhesives, J. Mater. Sci.: Materials in Electronics. 27 (2016) 3540–3548. doi:10.1007/s10854-015-4189-3.

[38] G. Naja, P. Bouvrette, S. Hrapovic, J.H.T. Luong, Raman-based detection of bacteria using silver nanoparticles conjugated with antibodies, Analyst, 132 (2007) 679–686. doi:10.1039/b701160a.

[39] A.K. Mishra, N.H. Kim, D. Jung, J.H. Lee, Enhanced mechanical properties and proton conductivity of Nafion-SPEEK-GO composite membranes for fuel cell applications, J. Membrane. Sci. 458 (2014) 128–135. doi:10.1016/j.memsci.2014.01.073.

[40] K.K.H. De Silva, H. Huang, R.K. Joshi, M. Yoshimura, Chemical reduction of graphene oxide using green reductants, Carbon. 119 (2017) 190–199. doi:10.1016/j.carbon.2017.04.025.

[41] Z.J. Li, B.C. Yang, S.R. Zhang, C.M. Zhao, Graphene oxide with improved electrical conductivity for supercapacitor electrodes, Appl. Surf. Sci. 258 (2012) 3726–3731.doi:10.1016/j.apsusc.2011.12.015.

[42] R. Batul, T. Tamanna, A. Khaliq, A. Yu, Recent progress in the Biomaterials applications of polydopamine nanostructures, 7 (2017) 1204–1229. doi:10.1039/c7bm00187h.

[43] M. Cui, S. Ren, H. Zhao, Q. Xue, L. Wang, Polydopamine coated graphene oxide for anticorrosive reinforcement of water-borne epoxy coating, Chem. Eng. J. 335 (2017) 255–266. doi:10.1016/j.cej.2017.10.172.

[44] D. Ariono, I.G. Wenten, Heterogeneous structure and its effect on properties and electrochemical behavior of ion- exchange membrane Heterogeneous structure and its effect on properties and electrochemical behavior of ion-exchange membrane, Mat. Res. Express. 4 (2017) 1-12. doi:10.1088/2053-1591/aa5cd4.

[45] Z. Xi, Y. Xu, L. Zhu, Y. Wang, B. Zhu, A facile method of surface modification for hydrophobic polymer membranes based on the adhesive behavior of poly (DOPA) and poly (dopamine), J. Membrane Sci. 327 (2008) 244-253. doi:10.1016/j.memsci.2008.11.037.

[46] H. Yang, Y. Lan, W. Zhu, W. Li, D. Xu, J. Cui, D. Shen, G. Li, Polydopamine-coated nanofibrous mats as a versatile platform for producing porous functional membranes, J. Mater. Chem. 22 (2012) 16994-17001. doi:10.1039/c2jm33251e.

[47] C. Fernandez-Gonzalez, B. Zhang, A. Dominguez-ramos, R. Ibañez, A. Irabien, Y. Chen, Enhancing fouling resistance of polyethylene anion exchange membranes using carbon nanotubes and iron oxide nanoparticles, Desalination. 411 (2017) 19–27. doi:10.1016/j.desal.2017.02.007.

[48] Y. He, J. Wang, H. Zhang, T. Zhang, B. Zhang, S. Cao, J. Liu, Polydopamine-modified graphene oxide nanocomposite membrane for proton exchange membrane fuel cell under anhydrous conditions, J. Mater. Chem. A. 25 (2014) 9548-9558 doi:10.1039/c3ta15301k.

[49] M. Porozhnyy, P. Huguet, M. Cretin, E. Safronova, V. Nikonenko, C. Umr, C.C.P.E. Bataillon, M. Cdx, Mathematical modeling of transport properties of proton-exchange membranes containing immobilized nanoparticles, Int. J. Hydrogen Ener. 41 (2016) 15605–15614. doi:10.1016/j.ijhydene.2016.06.057.

[50] S.M. Hosseini, A. Gholami, P. Koranian, M. Nemati, S.S. Madaeni, A.R. Moghadassi, Electrochemical characterization of mixed matrix heterogeneous cation exchange

membrane modified by aluminum oxide nanoparticles: Mono/bivalent ionic transportation, J. Taiwan Inst. Chem. Eng. 45 (2014) 1241–1248. doi:10.1016/j.jtice.2014.01.011.

[51] N. Kononenko, V. Nikonenko, D. Grande, C. Larchet, L. Dammak, M. Fomenko, Y. Volfkovich, Porous structure of ion exchange membranes investigated by various techniques, Adv. Colloid. Interface Sci. 246 (2017) 196–216. doi:10.1016/j.cis.2017.05.007.

[52] J. Kamcev, D.R. Paul, B.D. Freeman, Effect of fixed charge group concentration on equilibrium ion sorption in ion exchange membranes, J. Mater. Chem. 5 (2017) 4638–4650. doi:10.1039/C6TA07954G.

[53] R. Kiyono, G.H. Koops, M. Wessling, H. Strathmann, Mixed matrix microporous hollow fibers with ion-exchange functionality, 231 (2004) 109–115. doi:10.1016/j.memsci.2003.11.008.

[54] L.X. Tuan, D. Mertens, The two-phase model of structure microheterogeneity revisited by the study of the CMS cation exchange membrane, Desalination. 240 (2009) 351–357. doi:10.1016/j.desal.2007.10.098.

[55] S. Moshtarikhah, N.A.W. Oppers, M.T. de Groot, J.T.F. Keurentjes, J.C. Schouten, J. van der Schaaf, Nernst–Planck modeling of multicomponent ion transport in a Nafion membrane at high current density, J. Appl. Electrochem. 47 (2017) 51–62. doi:10.1007/s10800-016-1017-2.

[56] O.A. Demina, N.A. Kononenko, I. V Falina, New Approach to the Characterization of Ion Exchange Membranes Using a Set of Model Parameters, Pet. Chem. 54 (2014) 515–525. doi:10.1134/S0965544114070032.

[57] W. Zhang, P. Wang, J. Ma, Z. Wang, H. Liu, Investigations on electrochemical properties of membrane systems in ion-exchange membrane transport processes by electrochemical impedance spectroscopy and direct current measurements, Electrochim. Acta. 216 (2016) 110–119. doi:10.1016/j.electacta.2016.09.018.

[58] K.J. Chae, M. Choi, F.F. Ajayi, W. Park, I.S. Chang, I.S. Kim, Mass Transport through a Proton Exchange Membrane (Nafion) in Microbial Fuel Cells, Energ. Fuel. 22 (2008) 169–176. doi:10.1021/ef700308u.

[59] A.A. Moya, E. Belashova, P. Sistat, Numerical simulation of linear sweep and large amplitude ac voltammetries of ion-exchange membrane systems, J.Membrane. Sci. 474 (2015) 215–223. doi:10.1016/j.memsci.2014.10.006.

[60] E. Fontananova, W. Zhang, I. Nicotera, C. Simari, W. Van Baak, G. Di, E. Curcio, E. Drioli, Probing membrane and interface properties in concentrated electrolyte solutions, J. Membrane. Sci.459 (2014) 177–189. doi:10.1016/j.memsci.2014.01.057.

[61] W. Cai, J. Yan, T. Hussin, J. Liu, Nafion-AC-based asymmetric capacitive deionization, Electrochim. Acta. 225 (2017) 407–415. doi:10.1016/j.electacta.2016.12.069.

[62] T.W. Xu, Y. Li, L. Wu, W.H. Yang, A simple evaluation of microstructure and transport parameters of ion-exchange membranes from conductivity measurements, Sep. Purif. Technol. 60 (2008) 73–80. doi:10.1016/j.seppur.2007.07.049.

[63] A.B. Yaroslavtsev, E.Y. Safronova, A.A. Lysova, S.A. Novikova, I.A. Stenina, V.I. Volkov, Ion conductivity of hybrid ion exchange membranes incorporating nanoparticles, Desalin. Water. Treat. 35 (2011) 202-208.

Fig. 1. SEM micrographs of the AgNPs (a), the graphene oxide sheet, GO (b), and the different proportions of $AgNO_3$ and GO used: Ag_1GO (c), Ag_3GO (d), Ag_6GO (e) and Ag_9GO (f).

Fig. 2. Characterization of NCs: Diffractograms (a), Raman (b) and Infrared spectra (c) obtained from different proportions of $AgNO_3$ and GO. In addition, of the number of stacked layers of GO in NCs and the number of AgNPs that were obtained by UV-vis analyzes (d).

Fig. 3. Scheme of the preparation process of AgNPs (a), synthesis of the AgNPs-GO nanocomposite (b) and the preparation of pda coating on a GO sheet (c).

Fig. 4. Superficial and transverse micrographs of the Nafion and Ultrex modified membranes. Pristine Nafion and Ultrex (a, a´, e, e´, respectively); Nafion and Ultrex with pda (b, b´,f, f´, respectively); Nafion and Ultrex with pdaGO (c, c´,g, g´, respectively) and Nafion and Ultrex with pdaNC (d, d´,h, h´, respectively).

Fig. 5. Superficial topography and 3D images obtained from AFM analyzes for the Nafion and Ultrex modified membranes. Pristine Nafion and Ultrex (a, a´, e, e´, respectively); Nafion and Ultrex with pda (b, b´,f, f´, respectively); Nafion and Ultrex with pdaGO (c, c´,g, g´, respectively) and Nafion and Ultrex with pdaNC (d, d´,h, h´, respectively).

Fig. 6. Dynamic contact angle graphs showing the filterability the water behavior of the modified Nafion (a) and Ultrex membranes (b). In addition, the tendency to hydrophilicity of the modified membranes is shown (c).

Fig. 7. Nyquist diagrams for the modified membranes of the Nafion and ultrex modified membranes in acid 0.1 M H_2SO_4 (a and b, respectively) and in neutral 0.5 M NaCl media (c and d, respectively). In addition, zooms are shown at the high frequency limit where the behavior of the resistance of the membranes in contact with the solution is observed (R_{m+s}).

Fig. 8. Interfacial and membrane resistance (a, b, e and f) and conductivity (c, d, g and h) values for the modified Nafion and Ultrex membranes different degrees of modification of Nafion and Ultrex in acid 0.1 M H_2SO_4 (a-d, respectively) and neutral 0.5 M NaCl (e-h, respectively) media.

Fig.9. Micrographs showing the anti(bio)fouling capacity of the pristine and modified membranes that were immersed in inoculum obtained from municipal waste water.

Table 1. Roughness and height parameters obtained from AFM analysis of the modified membranes.

Membrane	RMS Surface roughness (nm)	Height (nm)
Nctrl	5.6±1.6	75±15
Npda	26±1.4	208±31
NpdaGO	37±4.7	165±33
NpdaNC	7±0.2	21±5
	RMS Surface roughness (μm)	**Height (μm)**
Uctrl	0.4±0.01	1.5±0.3
Upda	0.7±0.3	2.2±1
UpdaGO	0.1±0.07	0.8±0.2
UpdaNC	0.2±0.1	1.2±0.5

Table 2. Physicochemical properties of the modified Nafion and Ultrex membranes.

Membrane	% Water uptake	IEC (meq/g)	FIC (meq/g)	Contact angle (ø)
Nctrl	41.2±8	2.5±0.9	5.9±1	94±6
Npda	73±3.5	4.2±0.4	6.9±1	55±5
NpdaGO	63±2.4	4±0.4	6.8±2.7	63±14
NpdaNC	78±16	6±0.9	7.7±1	47±4
Uctrl	36±4	1.4±0.1	4±0.8	78±2
Upda	23±3	1.2±0.02	5.2±0.7	19±8
UpdaGO	21±1	1.1±0.1	5.6±0.4	40±3
UpdaNC	25±2	1±0.05	4.1±0.5	34±4

*IEC: ionic exchange capacity, FIC: fixed ion concentration, Nctrl and Uctrl: pristine membranes, Npda and Upda: Nafion and Ultrex with pda, NpdaGO and UpdaGO: Nafion and Ultrex with GO adhered by pda, NpdaNC and UpdaNC: Nafion and Ultrex with AgNPs-GO adhered by pda adhesive.

Table 3. Electrochemical properties of the modified Nafion and Ultrex membranes.

Membrane	Membrane Potential (V)	t^1m	P_s	Donnan Potential (V)	RI (ohms/cm^2)	Conductivity (μS/cm)	I_{lim} (μA/cm^2)
Nctrl	0.03±0.002	0.7±0.02	0.6±0.03	-0.25±0.03	26±6	12±3	4±0.2
Npda	0.04±0.004	0.8±0.03	0.76±0.04	-0.1±0.02	15±7	23±1	1.3±0.4
NpdaGO	0.043±0.003	0.9±0.03	0.78±0.05	-0.15±0.02	3.5±0.03	84±0.9	28±3.5
NpdaNC	0.05±0.001	0.9±0.01	0.85±0.02	-0.08±0.07	13.5±3	24±6	22±0.7
Uctrl	0.047±0.004	0.9±0.03	0.84±0.05	-0.05±0.05	71±14	81±17	3±0.2
Upda	0.06±0	0.98±0	0.98±0	-0.11±0.03	69±1	81±16	2.5±0.7
UpdaGO	0.06±0	0.981±0	0.98±0	-0.12±0.04	75±2	75±2	18±4
UpdaNC	0.05±0.001	0.92±0.02	0.88±0.03	-0.09±0.02	79±10	71±9	43±3.5

*t^1m: transport number, Ps: permeselectivity, RI: ohmic drop, I_{lim}: limiting current. Nctrl and Uctrl: pristine membranes, Npda and Upda: Nafion and Ultrex with pda, NpdaGO and UpdaGO: Nafion and Ultrex with GO adhered by pda, NpdaNC and UpdaNC: Nafion and Ultrex with AgNPs-GO adhered by pda adhesive.

HIGHLIGHTS

- *Cationic exchange membranes were modified with AgNPs-GO nanocomposites and polydopamine.*
- *The physicochemical and conductivity properties of modified Nafion were enhanced.*
- *The modified Ultrex improved its conductivity.*
- *The anti(bio)fouling properties of both modified membranes were improved.*

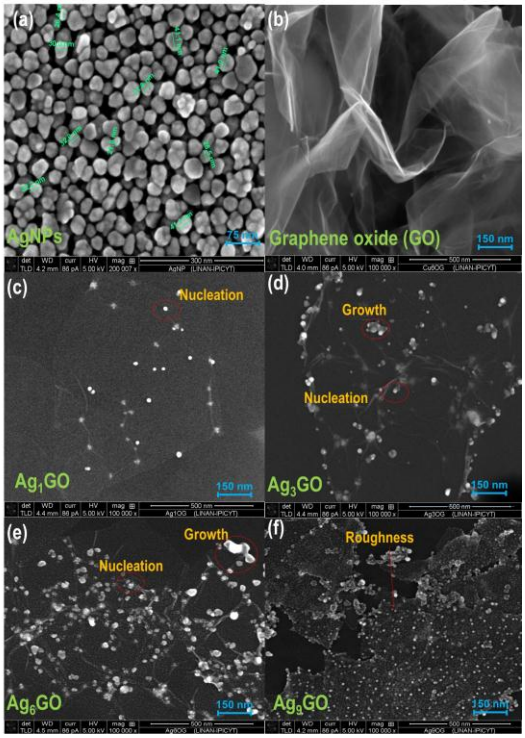

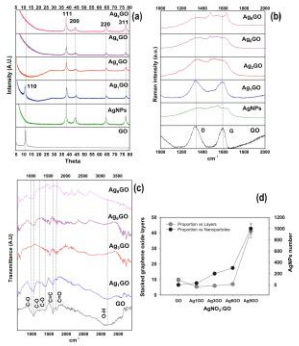

(a) AgNPs

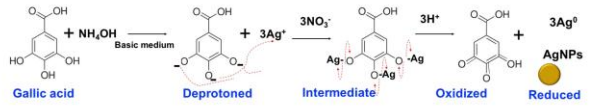

(b) Synthesis of the AgNPs-GO nanocomposite

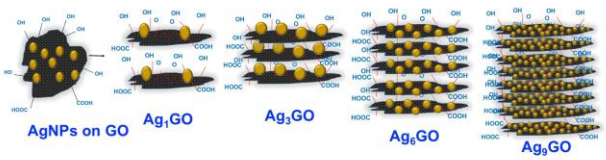

(c) Polydopamine (pda) on GO sheet

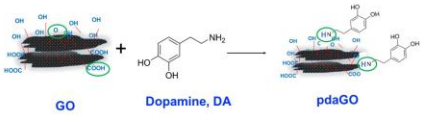

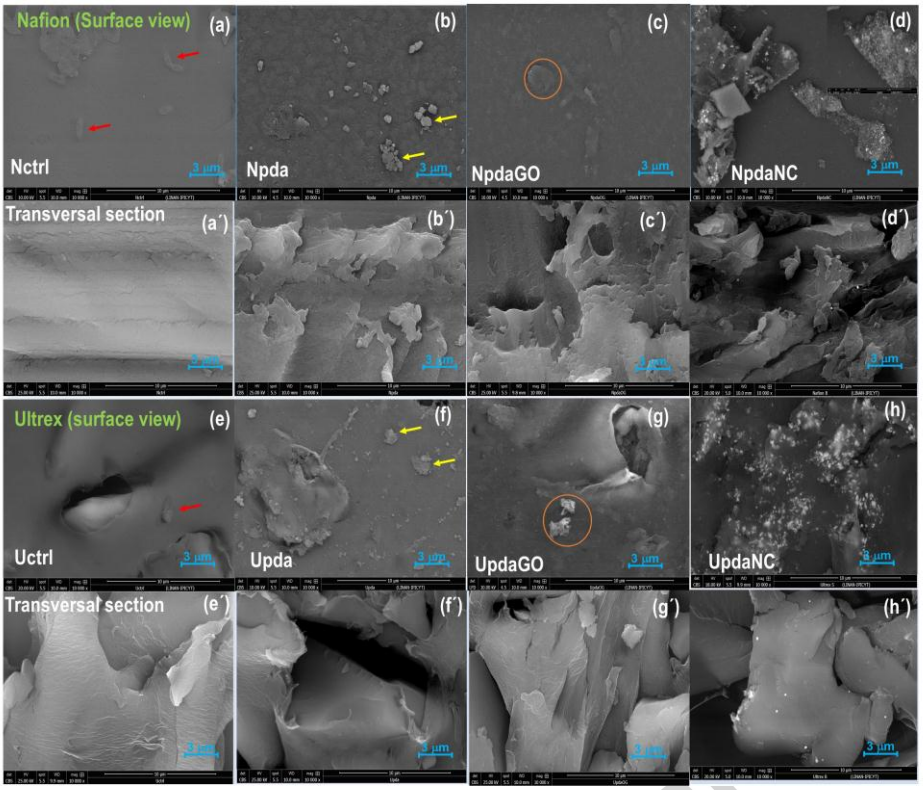

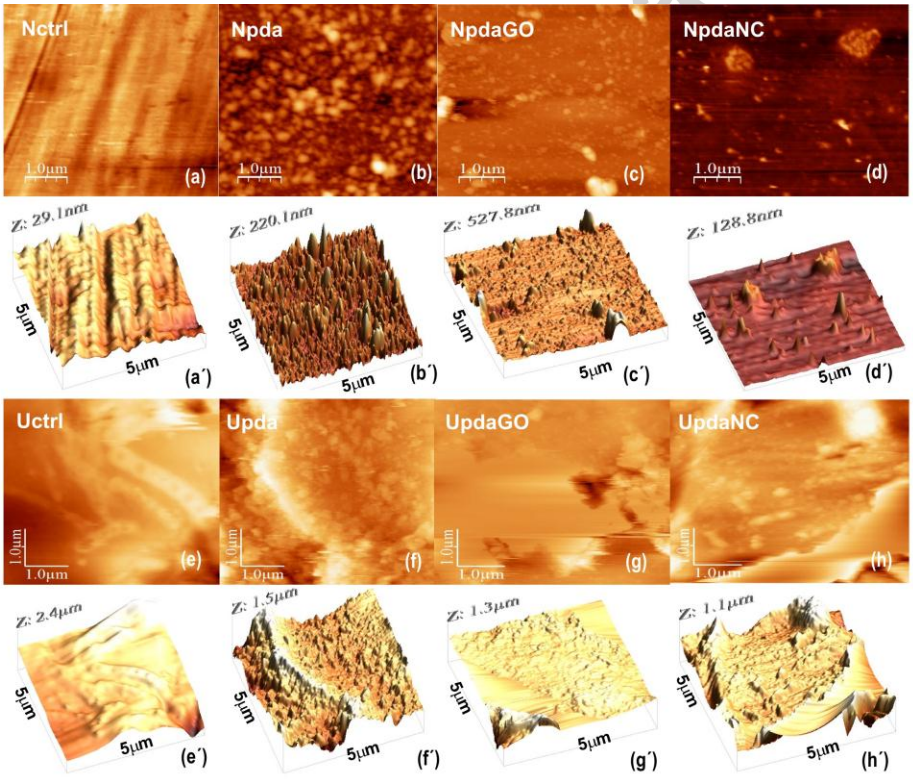

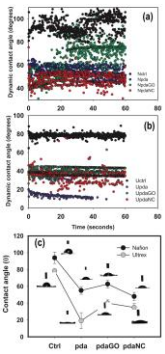

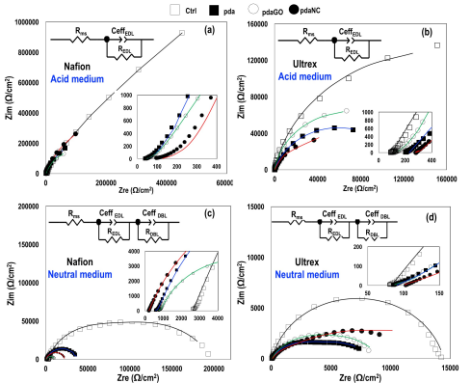

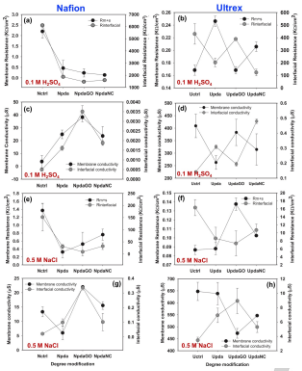

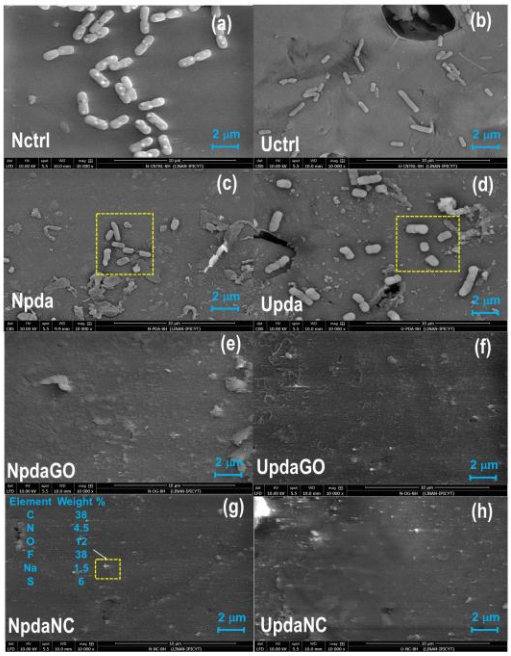

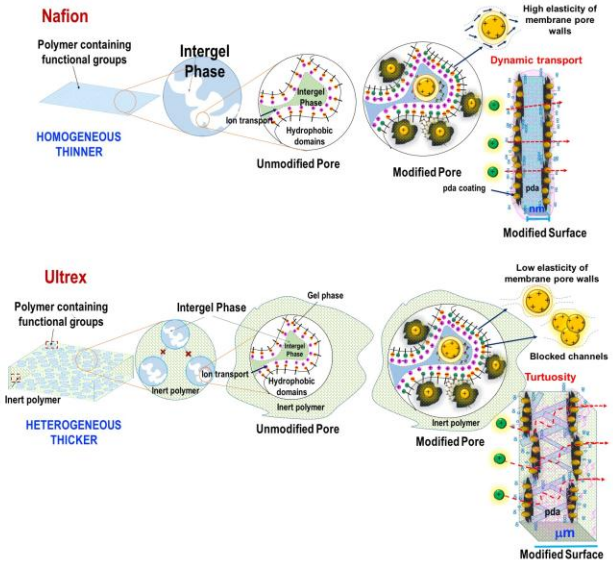

GRAPHICAL ABSTRACT